

1 Introduction

SuperDARN radars use pulses of HF energy to detect convective motion in the ionosphere. The range to a particular target is deduced from the timing between transmit and receive versions of the transmit pulse sequence. Various equations for the ground range, elevation angle and virtual height appear in the literature for flat Earth and spherical geometries. The spherical Earth geometry and associated equations and assumptions are collected below.

2 Slant and ground range

Assume that the EM radiation transmitted and received by an antenna array of an over-the-horizon, HF radar travels at the speed of light in vacuum, c . A schematic of the situation is shown in Figure 1.

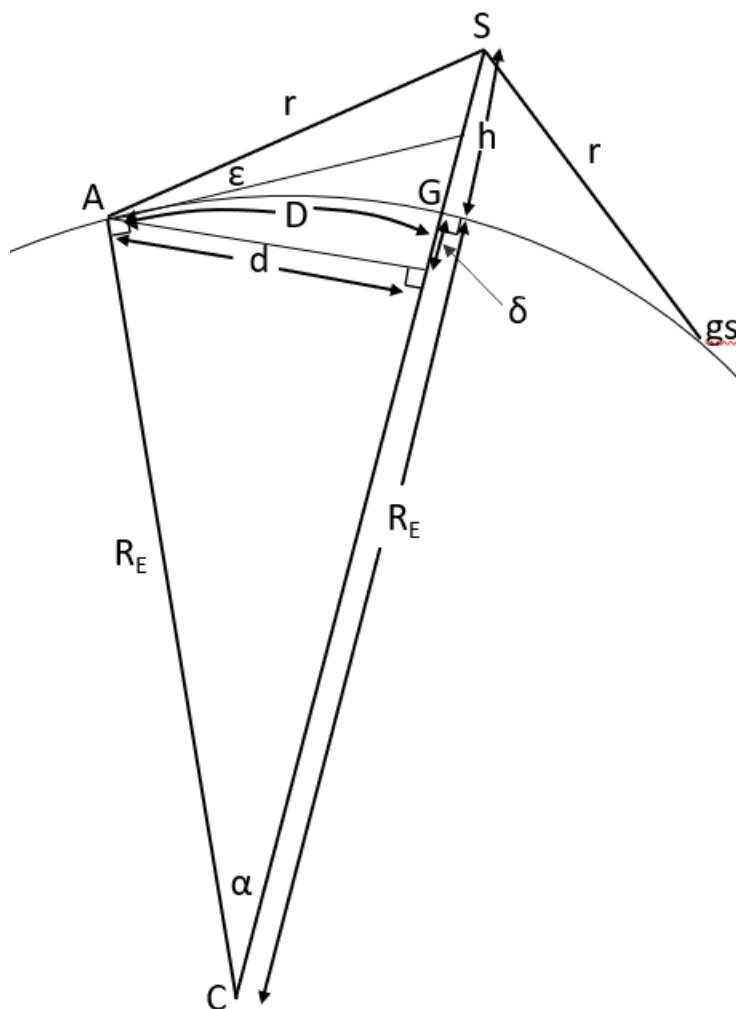


Figure 1: Schematic of HF ray path originating from an antennae array, A up to virtual height, h at point S in an Earth curvature context.

The Earth centre is at point C . The radar antennae are located at A , an Earth radius, R_E , from C . The 0.5 hop, ionosphere scatter location is located at point S , a slant range r from A . Ground scatter from a slant range distance of $2r$ has imposed doppler effects from the ionosphere dynamics at slant range, r .

The radiation elevation angle is ϵ so that the angle at A subtended by slant range r and Earth radius R_E is $(90 + \epsilon)$ degrees. The virtual height of S from the ground is h . The triangle, ASC subtends an angle, α at

Earth's centre.

The arc length distance from the antennae, A , to the ground range of the backscatter location, G , is $D = R_E \alpha$. The straight line distance (through the Earth) from the antennae located at A to the point directly below S (and G) is d where this straight line of length d and the Earth radius, R_E , meet at 90 deg as shown. The virtual height, h is measured from the ground so there is an additional distance below ground, δ that is important for published equations of the ground scatter range. Right angle triangle ASG has hypotenuse of length r and sides of length d and $(h + \delta)$.

For SuperDARN radars, ground range distance, D is of interest to provide latitude and longitude locations of radiation beam and range gate coordinates.

Timing in the radar provides the slant range, r . However, additional evidence must be provided in order to ascertain the HF scatter location. The 0.5 hop ionosphere scatter location is S . Ground scatter may be from a slant range distance of $2r$. Multiple hop propagation modes are also possible.

3 Ground scatter

Assume a spherical Earth, scatter from the ground at a slant range distance of $2r$ via the ionosphere point, S . We wish to determine the ground distance, D . Bristow et al., (1994) gave the equation

$$D = R_E \sin^{-1} \left[\frac{\sqrt{\frac{R_E^2}{4} - h^2}}{R_E} \right] \quad (1)$$

We can see that the ground distance D in Eqn 1. is an approximation and the accuracy depends on the length, δ in Figure 1. In order to see the origin of Eqn 1. and how this approximation arises, the three relevant relations from Figure 1 are

$$\sin \alpha = \frac{d}{R_e} \quad (2)$$

$$D = R_e \alpha \quad (3)$$

$$r^2 = d^2 + h^2 \quad (4)$$

Eqn 4 is the approximation as h is the virtual height from S to the ground along a radius, R_E , which is smaller than the real length from S down to the perpendicular intersection of d with the radius, R_E , by an amount, δ .

4 Ionosphere scatter

Range calculations that involve the elevation angle, ε , to 0.5 hop scatter location, S , involve triangles in Figure 1 and the sine and cosine rules.

Ponomarenko et al. (2018) have an equation that relates the virtual height, h and the elevation angle, ε . This may be obtained from the cosine rule using the angle at A as

$$(R_E + h)^2 = R_E^2 + r^2 - 2R_E r \cos (90 + \varepsilon) \quad (5)$$

or since $\cos(90 + \varepsilon) = -\sin \varepsilon$

$$(R_E + h)^2 = R_E^2 + r^2 + 2R_E r \sin \varepsilon \quad (6)$$

Therefore,

$$h = \sqrt{R_E^2 + r^2 + 2r R_E \sin \varepsilon} - R_E \quad (7)$$

which is Eqn. 10 of Ponomarenko et al., (2018). Eqn 7 is also coded as `calc_virtual_height` in `rpos.v2.c` where the slant range, r , is written as `r * 0.5/hop`.

An expression for the slant range, r , can be obtained from Eqn 6. Using the quadratic formula to solve for r gives

$$r = -R_E \sin \varepsilon \pm \sqrt{R_E^2 \sin^2 \varepsilon - R_E^2 + (R_E + h)^2} \quad (8)$$

and taking the positive solution yields

$$r = [(R_E + h)^2 - R_E \cos^2 \varepsilon]^{1/2} - R_E \sin \varepsilon \quad (9)$$

which is the Eqn 1. of Andre et al., (1998).

Additional formulae involving the elevation angle, ε , may be obtained using the sine rule on the triangles in Figure 1. However, the elevation angle is rarely used in SuperDARN with difficulties in measurements of this quantity discussed by Ponomarenko et al. (2018) and Chisham et al. (2021). Therefore, the ground range, D is deduced from the range to the scatter, r , plus an assumed virtual height, h and propagation mode. The geometry also precludes the large elevation angle, Pedersen propagation mode.

The cosine rule from triangle ASC and using angle α in Figure 1 gives

$$r^2 = R_E^2 + (R_E + h)^2 - 2R_E(R_E + h) \cos \alpha \quad (10)$$

Therefore,

$$-\cos \alpha = \frac{(r + R_E)(r - R_E) + (R_E + h)^2}{2R_E(R_E + h)} \quad (11)$$

Solve for α and then use $D = R_E \alpha$. Eqn 11 is coded as `calc_ground_range` in `rpos_v2.c` where the slant range, r , is written as `r * 0.5/hop`. A comparison of the ground range, D , using the approximation of Eqn 1 and Eqn 11 is shown in Figure 2.

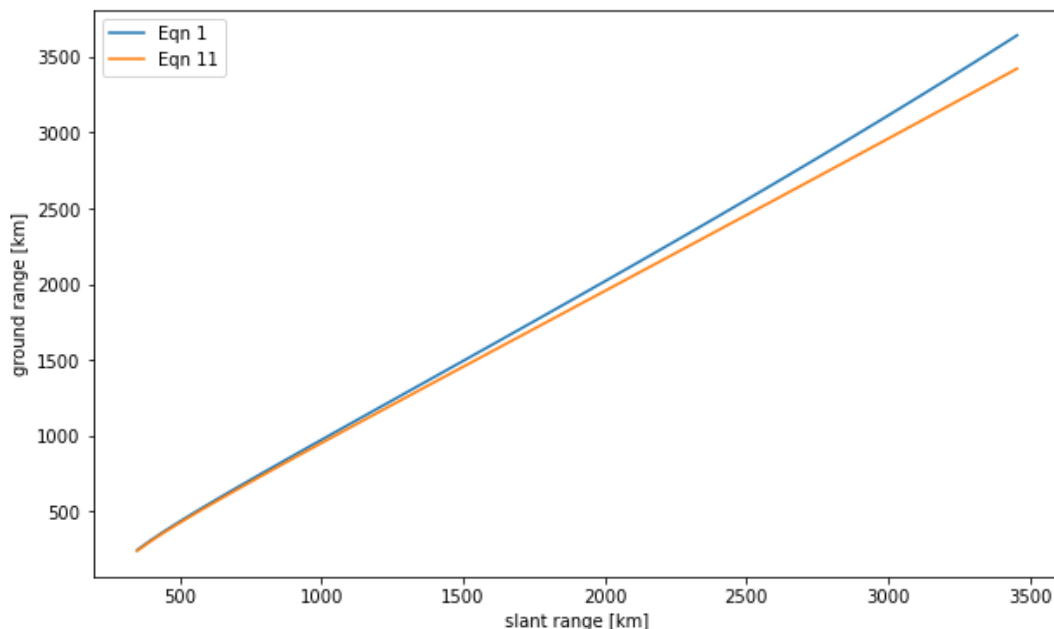


Figure 2: Comparison of Eqn 1 and Eqn 11 for ground range calculation, D in Figure 1.

5 SuperDARN range variables

A list of SuperDARN datamap variables and definitions is available at <https://superdarn.github.io/rst/superdarn/src.doc/rfc/0>

The variables relevant to beam and range gate calculations are as follows

- `bmazm`: beam azimuth
- `bmnum`: beam number
- `frang`: distance to first range (km)

- lagfr: the lag to the first range (microsec)
- nrang: number of ranges
- rsep: range separation (km)
- rxrise: receiver rise time (microsec)
- smsep: data sample separation (microsec)
- txpl: transmit pulse length (microsec)

Quite often some of these variables have the same value, For example, $txpl=smsep$. The slant range, r , is calculated in `cnvtcoord.c` in the function `slant_range` as follows.

```
/* Calculate the lag to first range gate in microseconds */
lagfr=frang*20/3;
```

For example, if $frang=180$ km then the time taken for the EM pulse to travel 180 km and back to the receiver is $lagfr = 2*(180,000)/c * 1e6$ (microsec). Using $c=3e8$ we have $lagfr = 2*1000*1e6/3e8 * frang$ (km), which is $20/3*frang$. Therefore, $20/3$ is a conversion factor between distance (km) to time (microsec). The $lagfr$ variable is a SuperDARN datamap variable.

```
/* Calculate the sample separation in microseconds */
smsep=rsep*20/3;
```

The quantity $rsep$ (km) is the distance between range gates, set by the data sample interval, $smsep$. The $smsep$ variable is a SuperDARN datamap variable.

```
/* Return the calculated slant range [km] */
return (lagfr-rxris+(range_gate-1)*smsep+range_edge)*0.15;
```

The 0.15 value is $3/20$, the conversion from time (microsec) to distance (km) assuming speed of light in vacuum is $3e8$ m/s. Therefore, all quantities in the brackets have units of microsec and comprise all time components for the EM pulse to travel the distance between the antenna and scatter location.

The assumptions used for the equations are

- EM pulses have speed $c=3e8$
- The virtual height is used for h
- Straight line EM ray propagation to form the triangles of Figure 1.
- Adjustments to slant range, r , for ionosphere backscatter when the EM ray-path is perpendicular to the ambient magnetic field is not included
- Large elevation angle, Pedersen propagation mode is excluded
- The number of ground hops is known
- Distinction between ground and ionosphere scatter is known.

C. L. Waters
 Newcastle, New South Wales, Australia
 July 2023

6 References

Andre, D., G. Sofko, K. Baker, J. MacDougall (1998) SuperDARN interferometry: Meteor echoes and electron densities from ground scatter, *J. Geophys. Res.*, 103, 7003-7015.

Bristow, W.A., R.A. Greenwald and J.C. Samson (1994), Identification of high-latitude acoustic gravity wave sources using the Goose Bay HF radar, *J. Geophys. Res.*, 99(A1), 319–331, doi:10.1029/93JA01470.

Chisham, G., A. G. Burrell, A. Marchaudon S. G. Shepherd, E. G. Thomas and P. V. Ponomarenko, (2021), Comparison of interferometer calibration techniques for improved SuperDARN elevation angles, *Polar Science* 28, 100638, <https://doi.org/10.1016/j.polar.2021.100638>.

Ponomarenko, P.V., J.-P. St.-Maurice, K. A. McWilliams, (2018), Calibrating HF radar elevation angle measurements using E layer backscatter echoes, *Radio Science*, 53, 1438–1449, <https://doi.org/10.1029/2018RS006638>.